PETROLEUM SOCIETY
CANADIAN INSTITUTE OF MINING, METALLURGY & PETROLEUM

PAPER 2004-008

How much oil you can get from CHOPS

GANG HAN, MIKE BRUNO
Terralog Technology Inc.

MAURICE B. DUSSEAULT
University of Waterloo

This paper is to be presented at the Petroleum Society's 5th Canadian International Petroleum Conference (55th Annual Technical Meeting), Calgary, Alberta, Canada, June 8 – 10, 2004. Discussion of this paper is invited and may be presented at the meeting if filed in writing with the technical program chairman prior to the conclusion of the meeting. This paper and any discussion filed will be considered for publication in Petroleum Society journals.

Abstract

Cold Heavy Oil Production with Sand (CHOPS) has been applied with very good success to enhance heavy oil production in Canada, China, Venezuela, and Kazakhstan. Based on existing laboratory and field information and case histories, the most important physical processes enhancing cold production have been reviewed, summarized, and quantified.

Several sanding models are developed, including a new porosity cap model for failure propagation as well as a semi-analytical elastoplastic stress model coupled with an unsteady pressure model for foamy oils. The mechanisms for oil rate enhancement by CHOPS, such as porosity and permeability enhancement that arise from sand removal, propagation of the elastoplastic (remolded) zone, increase of oil velocity relative to the matrix, and the effects of foamy oil behavior, are quantitatively described and compared.

The proposed model can be applied to predict how much additional oil one might expect for a given amount of produced sand. It might also serve as a tool for optimizing cold heavy oil production while nevertheless keeping the sand flux at a low level, which could reduce operating expenses such as limiting sand disposal costs.

Introduction

There may be more than 6 trillion barrels of heavy oil on Earth [(1)], compared to 1.75-2.3 trillion barrels of conventional oil, over 40% of which has already been produced [(2)]. Because of high viscosity, primary recovery factors for heavy oils are generally low; if the viscosity is higher than 10,000-20,000 cP in situ and the permeability less than 5 Darcy, it appears that commercial recovery using any conventional non-thermal method is not possible. With careful design and implementation, various thermal recovery schemes can be effective, but high operational costs restrict their applicability.

Though it has been long recognized that "…the maximum recovery of oil from an unconsolidated sand is directly dependent upon the maximum recovery of the sand itself…." [(3)], CHOPS was not widely implemented with commercial success until advanced pumping systems (such as the progressive cavity pumps) were perfected in the late 1980s for slurries containing sand.

Since then, because of reasonable recovery factors (~15-20%), production rates (20-300 bbl/day), effective sand handling and disposal, and no heat costs, CHOPS has grown to provide more than 20% of Canada's oil. In 2002, Canada's oil production from all sources was ~ 2.9×10^6 b/d, of which more than 600,000 b/d was CHOPS production. Heavy oil reservoirs

suitable for CHOPS are located in unconsolidated or weakly consolidated sands where sand mobilization can be easily triggered and sand influx sustained for the productive life of the well.

Because of several unique characteristics of unconsolidated heavy oil reservoirs, well productivity may be 10-20 times higher in CHOPS wells than predicted by conventional Darcy's law flow equations [4]. The mechanisms responsible for the enhanced production rate in CHOPS are [5]:

- Porosity and permeability are enhanced as sand is removed from the formation, along with any mechanical skin that may have developed;
- The oil flow velocity relative to fixed coordinates is increased if the matrix is partially mobilized, therefore production rate increases, as predicted from Darcy's law;
- Foamy oil behavior, where solution gas stays as bubbles and a continuous gas phase does not form, contributes to flow enhancement;
- Increased compressibility and porosity dilation occur, leading to easier formation compression and compaction drive; and,
- Sand removal leads to vertical stress concentrations and lateral stress reductions, causing shear dilation, continued sand destabilization, and plastic extrusion of sand to the wellbore.

Experimental evidence indicates that the first two mechanisms could increase the oil flow rate by as much as 5 to 50 times [6]. If skin damage is present in conventional oil wells, allowing occasional sand bursts during production or using a workover method that deliberately produces some sand may increase productivity substantially. An average rate increase of 30-40% in North Sea fields was observed after implementing this approach, and in some individual wells, rate increases greater than 80% were achieved in high production rate wells (1000 – 3000 m^3/day). In this case, the mechanism is dominated by the removal of mechanical skin near well-bore [7].

Most heavy oils are gas-saturated in situ, i.e. the bubble point pressure is at or very close to the pore pressure. However, because of kinetic constraints in high viscosity liquids, gas bubble nucleation is difficult and growth rate of nucleated bubbles is suppressed [8]. Hence, gas bubbles apparently remain in a "foamy" phase without coalescence into a continuous gas phase in the near wellbore region. CHOPS production records from Alberta (public-domain production records from the Alberta Energy Utilities Board) often show a constant gas-to-oil ratio for many years, proving that a continuous phase has not been generated to more rapidly deplete the solution gas around the well or in the far-field.

The expansion of gas bubbles as they flow down the pressure gradient to the well accelerates heavy oil production, and is considered an essential part of CHOPS [9]. Also, gas bubbles help block pore throats, which is beneficial to CHOPS because it promotes sand destabilization through generation of high local pressure gradients. Because no continuous gas phase seems to be generated, CHOPS can be sustained for long well lives (up to 12-14 years in some cases) and continues as long as new and undisturbed unconsolidated sand reservoir can be destabilized. Interestingly, laboratory experiments have shown that the mobility of heavy oil does not increase with the presence of a dispersed bubble-in-oil phase alone [10-12]. It seems that substantial flow enhancement through bubble effects and "foamy flow" requires concomitant sand flux. The contribution of foamy oil behavior to recoverable oil could be on the order of 10% of OOIP [11], or a 50% increase in the productivity of a well over its life [13]. In Canadian heavy oil experience, CHOPS can achieve recovery factors exceeding 20% in appropriate reservoirs.

The enhancement figures discussed above are mainly based on empirical observations and laboratory tests where boundary conditions do not even closely resemble the field case. It would be advantageous if a consistent and relatively simple model based on physical processes could be developed to help predict such rate enhancements.

Some modeling developments have been made recently. However either steady-state fluid flow was assumed (e.g. Ref. 14) despite clear evidence that foamy oil behavior show strong time dependence, or a more complicated sanding propagation model was used (e.g. the wormhole model in Ref. 15) at the expense of simplicity and ease of mathematical solution.

In this research a simple conceptual sanding propagation model is proposed, based on which elastoplastic stress solutions in unconsolidated sands and unsteady pressure conditions in a "foamy oil" environment are developed and coupled to describe oil production enhancement by CHOPS.

Model Development

Conceptual Sanding Propagation Model

Because of physical complexity and the limitations of experimental conditions, failure propagation modes and mechanisms in continuous sand production remain controversial and unclear [15-18]. Nevertheless, we will develop a model based on an assumed difference in rock mechanical behavior between an elastic region and a region where elastoplastic behavior, including dilation, is taking place. Accordingly, the formation around a wellbore is divided into elastic and elastoplastic zones (Fig. 1) and the problem is treated axisymmetrically. This conceptual model is consistent with laboratory observations of sand production around cavities, such as Fig. 2 [19].

The boundary is defined by a critical radius (R_c), at which sand has just experienced shear failure, which is defined by a Mohr-Coulomb yield criterion based on the effective radial and tangential stresses (σ'_r, σ'_θ):

$$\sigma'_\theta = 2C_o \tan\beta + \sigma'_r \tan^2\beta \quad \text{.....(1)}$$

Here, C_o is the cohesive shear strength and β is the failure plane angle which is related to the friction angle (φ) through $\beta = \pi/4 + \varphi/2$. All parameters are understood to be effective stress parameters. The plastic boundary propagates outward from the well with continuous sand flow as some of the sand within the elastoplastic zone continues to be plucked out of the rock matrix by fluid flow. Hence, both the porosity (ϕ) and the critical radius (R_c) are time-variable and location-variable and should so be treated in analysis. To simplify the model, however, the porosity of the elastoplastic zone is treated as an average value, and like the critical radius, it is assumed to vary only with time:

$$\phi = \phi(t);\ R_c = R_c(t) \quad \text{.....(2)}$$

Outside the critical radius ($r > R_c$), the porosity is assumed to be constant:

$$\phi = \phi_i \quad \text{.....(3)}$$

These simplifications would appear to be reasonable for unconsolidated sand as the porosities and permeabilities of those reservoirs are usually high (e.g. $\phi_i > 25\%$, $k_i > 0.5$ Darcy). The sanding mass rate Q_{ms} can be assumed to be [20]:

$$Q_{ms} = Q_{ms}^{\ o}\left(1 - \frac{at}{1+bt}\right) \quad \text{.....(4)}$$

and thus the accumulated sand mass is

$$CS_{ms} = \int Q_{ms} dt = {Q_{ms}}^{o}\left[(1-\frac{a}{b})t + \frac{a}{b^2}\ln(1+bt)\right] \quad \text{..... (5)}$$

In these equations, ${Q_{ms}}^{o}$ is the initial sanding rate and a and b are empirical parameters that, in the absence of more rigorous treatments, must be determined through a calibration procedure. The values used in this article are listed in Table 1. For development convenience, we denote the volumetric sand rate as $Q_s = Q_{ms}/\rho_s$, the cumulative sand volume as $CS = CS_{ms}/\rho_s$, and the volumetric solid velocity per unit thickness of reservoir as $q_s = Q_s/h$. Note also that $q = Q/h$ represents the volumetric oil velocity per unit thickness.

Furthermore, assuming that the produced sand comes from sand removal from the elastoplastic zone,

$$\int_{R_w}^{R_c} [\phi - \phi_i] 2\pi r dr = q_s \quad \text{..... (6)}$$

Therefore

$$[\phi - \phi_i]\pi\left(R_c^{\,2} - R_1^{\,2}\right) = CS \quad \text{..... (7)}$$

which logically suggests that sand production is related to both the increase of porosity and the outward propagation of the critical radius. To calculate the permeability, the Carman-Kozeny model is used because of its simplicity [21]:

$$k(t) = \left(\frac{\phi}{\phi_i}\right)^3 \left(\frac{1-\phi_i}{1-\phi}\right)^2 k_i \quad \text{..... (8)}$$

It should be noted that any relationship between permeability and porosity may be used, as long as it is expressed as a continuous variable over the porosity range used.

Elastoplastic Effective Stress Model

In the elastoplastic zone, the velocities of fluid (v_f) and solid (v_s) can be expressed as:

$$v_f = -\frac{q}{2\pi r\phi} \quad \text{.....(9a)}$$

$$v_s = -\frac{q_s}{2\pi r(1-\phi)} \quad \text{.....(9b)}$$

The negative sign implies that fluid and solid flows are in a direction opposite to the definition of the radial coordinate r (Fig. 1). Introducing these into the modified Darcy's law gives

$$-\frac{\partial P}{\partial r} = \frac{\mu}{k}\phi(v_f - v_s) \quad \text{.....(10)}$$

which results in

$$\frac{\partial P_p}{\partial r} = \frac{\mu}{2\pi k}(q - \frac{\phi q_s}{1-\phi})\frac{1}{r} \quad \text{.....(11)}$$

Here, P_p represents the pore pressure in the elastoplastic zone.

Stress equilibrium in the zone requires that

$$\frac{\partial \sigma_r'}{\partial r} + \frac{\sigma_r' - \sigma_\theta'}{r} = -\frac{\partial P_p}{\partial r} \quad \text{.....(12)}$$

Substituting the effective tangential stress from the yield criterion (Eq. 1) and the pressure gradient (Eq. 11), the solution for the plastic stresses can be obtained:

$$\sigma_r'(r) = \frac{c_3}{\omega} r^{-\omega} + \frac{2C_o \tan\beta + \Gamma(t)}{\omega} \quad \text{.....(13)}$$

$$\sigma_\theta'(r) = \frac{c_3(1-\omega)}{\omega} r^{-\omega} + \frac{2C_o \tan\beta + (1-\omega)\Gamma(t)}{\omega} \quad \text{.....(14)}$$

where $\Gamma(t) = -\frac{\mu}{2\pi k}(q - \frac{\phi q_s}{1-\phi})$ is the only time variable, and $\omega = 1 - \tan^2\beta$. Since at the inner boundary ($r = R_1$) we neglect the existence of a supportive casing, the radial effective stress must be zero, i.e $\sigma_r'(R_1) = 0$, therefore a solution for the constant c_3 can be found:

$$c_3 = -\left(2C_o \tan\beta + \Gamma(t)\right)\cdot R_1^{\,\omega} \quad \text{.....(15)}$$

Hence at each specific time, stresses are determined in the plastic zone. Solutions for the elastic stresses, as well as the plastic radius (R_c), are presented in Appendix A. We note that the assumption of zero radial effective stress at the interior boundary is justified in practice because the matrix is mobile. Compensated neutron logging has confirmed that in CHOPS field cases the well casing is often surrounded by a high porosity remolded zone.

Foamy Oil Pressure Model

To analyze foamy oil behavior, fluid properties such as compressibility and density of foamy oil need to be analytically stipulated. With the assumption that the fluid formation volume factor (B_f) is not greatly influenced by pressure, the compressibility of heavy oil can be calculated by [3]

$$c_f = {B_f}\big/{P} \quad \text{.....(16)}$$

The value of B_f is between 0.25 and 0.4, and for an ideal gas, $c_f = 1/P$. Hence the density of foamy oil becomes

$$\rho_f = \rho_{fsat}\left(\frac{P}{P_{sat}}\right)^{B_f} \quad \text{.....(17)}$$

where ρ_{fsat}, P_{sat} are fluid density and pressure in the saturated state. The viscosity of heavy oil is assumed to be constant in this treatment, although it is known that a CH_4-saturated heavy oil at formation pressures is about 30-40% of the viscosity of the dead oil at standard room pressure.

Corresponding to the formation classification, two types of pressure systems are described. The first is for the elastoplastic zone where a highly compressible fluid flows through a somewhat compressible rock matrix while sand is being detached at some rate from the matrix,

$$\nabla\cdot\left(\rho_f \frac{k(t)}{\mu}\nabla P\right) = \phi(t) c_t \rho_f \frac{\partial P}{\partial t} \quad \text{.....(18)}$$

The second is for the elastic zone where a highly compressible fluid flowing through a slightly compressible but stable matrix of constant porosity:

$$\nabla\cdot\left(\rho_f \frac{k_i}{\mu}\nabla P\right) = \phi_i c_t \rho_f \frac{\partial P}{\partial t} \quad \text{.....(19)}$$

Substituting ρ_f from Eq. (17), Eqs. (18) and (19) can be rewritten as:

$$\nabla^2 P_p^{(1+B_f)} = \frac{1}{M}\frac{\partial P_p^{(1+B_f)}}{\partial t} \quad \text{.....(20)}$$

$$\nabla^2 P_e^{(1+B_f)} = \frac{1}{M_i}\frac{\partial P_e^{(1+B_f)}}{\partial t} \quad \text{.....(21)}$$

where $M = \frac{k}{\mu\left(\phi c_f + (1-\phi)c_s\right)}$, and $M_i = \frac{k_i}{\mu\left(\phi_i c_f + (1-\phi_i)c_s\right)}$.

Boundary conditions can be specified as follows: pressures at the inner (R_1) and outer boundary are constants,

$$P_p(R_1,t) = P_1;\ P_e(R_2,t) = P_2 \quad \text{.....(22)}$$

while the pressure and the fluid rate across the interface between plastic and elastic zones (R_c) are continuous:

$$P_p(R_c) = P_e(R_c);\ k\left.\frac{\partial P_p^{1+B_f}}{\partial r}\right|_{r=R_c} = k_i\left.\frac{\partial P_e^{1+B_f}}{\partial r}\right|_{r=R_c} \quad \text{.....(23)}$$

The mathematical solutions for this model are presented in Appendix B.

Calculation and Discussions

Since the volume of foamy oil is affected by an unsteady fluid pressure, the conventional concept of volumetric oil rate should be adjusted before any discussion can be entertained. Using Eq. (17), Darcy's equation can be expressed in the term of the mass rate (m_f):

$$m_f = \frac{2\pi k \rho_{fsat} r}{\mu(1+B_f)P_{sat}{}^{B_f}}\frac{dP_e^{(1+B_f)}}{dr} \quad \text{.....(24)}$$

Assuming the mass rate is constant and integrating r from R_c to R_2 results in

$$\frac{m_f}{\rho_{fsat}} = \frac{2\pi k}{\mu(1+B_f)\ln(R_2/R_c)}\frac{P_2^{(1+B_f)} - P_c^{(1+B_f)}}{P_{sat}{}^{B_f}} \quad \text{.....(25)}$$

The left side of this equation is the volume rate q_{sc} (per unit formation thickness), as oil density at the saturation pressure ρ_{fsat} is nearly the same as the density at surface.

Inputs and Procedures

Fig. 3 shows a typical oil and sand production history (36 months) of a CHOPS well in Edam area, east of Lloydminster heavy oil block in Saskatchewan, Canada [26]. The burial depths of sands are shallow at 400-500 m, with low formation pressures (3 - 4 MPa), porosities of 30-36%, and permeability of 0.5-3 Darcies, gravity of 10-25° API, viscosity of 50-50,000 mPa.s. Without significant sand production, the average vertical well produced at steady but slow oil rates of 3-4 m^3/d, while CHOPS leads production rate at least 10 times higher.

To determine the coefficients in Eqs. (4) and (5), three sanding rates are needed at three different times. It is recommended that data such as shown on the figure be fitted with a smooth exponential decay curve that is asymptotic to a base rate (about 1.5% sand in this case).

With input of the 14 parameters listed in Table 2, the critical radius is first determined at each time step. Then, the porosity and permeability are updated according to Eqs. (7) and (8), combined with the sanding history data in Table 1. Finally, the enhanced oil rate is determined and serves as an input to calculate a new critical radius for the next time step.

Effect of Porosity Enhancement and Sand Movement

To accommodate sand removal from the oil-bearing formation, both formation porosity and plastic radius will increase. Based on the models developed above, the propagation of the elastoplastic zone is described in Fig. 5, and the evolution of porosity and permeability in the zone are plotted in Fig. 6. The plastic radius propagation is restrained only by the outer boundary (i.e. $R_c < R_2$), and this can be set as large as desired, or equal to a value such as the drainage radius of wells in a pattern.

The treatment of porosity must be discussed further. In this model, it can only increase to the point where the formation starts to collapse, which is called a "porosity cap" in this paper. After porosity reaches this cap, produced sands can only originate from continued plastic zone growth. This is likely to be a reasonable approach when overlying layers of oil formation are strong enough to support the additional loads that are redistributed by the enlargement of the elastoplastic zone. The value of the porosity cap may depend on various factors such as reservoir rock initial cohesion, frictional strength in the yielded state, the strength of the overlying formation, and so on. A value of $\phi = 0.52$ is used hereafter, as this is approximately the porosity value at which angular sand becomes completely liquefied (grain-to-grain effective forces disappear).

Fig. 6 shows that after only 1.2 days the porosity indeed reaches the cap value, and the absolute permeability reaches a value of 25 Darcy in the elastoplastic zone within a radius of about 0.5 m. This indicates that a high porosity and high permeability zone of limited radial extent has indeed been created at the initial stage of sand production.

In Fig. 7, corresponding to the rapid increase of critical radius (R_c) during the initial sanding stage (Fig. 5), oil production after two months is enhanced to 1.7 times its "initial rate". The enhancement mainly results from two mechanisms: the increase of rock porosity and permeability due to sand detachment from rock matrix, and the increase of oil relative velocity from Darcy's law. Interestingly, if one manually fixes the sand relative velocity in Eq. (10) to zero, i.e. the sands flow very slowly and there is no change of a relative velocity effect, the oil enhancement varies little (dashed line in Fig. 7) from the one considering both mechanisms (solid line in Fig. 7). This demonstrates that the variation of formation transport properties with sand production plays a far more important role than the change of fluid relative velocity in raising oil production. We believe this is indeed the case once the high early sand production rate is passed (it is not unusual to have sand volumes of 30-40% of produced fluids volumes in the first few hours).

Effect of Plastic Radius Propagation

If no porosity cap is taken to restrain the porosity increase, the calculations show it could easily reach a value such as 0.82 after three days production, with a permeability of more than 100 Darcies (Fig. 8). This could be taken to reflect the generation of a fully liquefied zone just around the wellbore. However, the oil rate shows an increase of only 1.2 times with the enlargement of porosity, and it remains nearly the same after the first three days (Fig. 9). Obviously, this does not fit the production history shown in Fig. 3, where the oil production rate was increased by a factor of three. On the other hand, the

results demonstrate that besides the improvement of transport properties such as porosity and permeability by sand production, there may be other important mechanisms for oil enhancement, including propagation of the plastic zone where low pressures and high permeabilities give the effect of wellbore enlargement. As shown in Fig. 5, this zone can be more than 8 times larger than the initial value at this time.

Effect of Foamy Oil Behavior

The main difference between sand production in a conventional oil reservoir and a heavy oil reservoir is the behavior of the fluid phase. Based on the developed models and parameters listed in Table 1, the contribution of foamy oil behavior to oil enhancement in a CHOPS well is quantified and plotted in Fig. 10. The foamy behavior, characterized as bubble growth, compressibility increase and density reduction, creates a significant increase in oil production. For cases with strong foamy behavior (e.g. $B_f = 0.4$ in Fig. 10) the oil production rate is multiplied by as much as 3.3. Even for the less foamy oil (e.g. $B_f = 0.1$ in Fig. 10), the production rate can be 3 times higher than initially, while without the presence of foamy oil the oil production is at most doubled.

These results now match fairly well the production history of the CHOPS well shown in Fig. 3, where oil rate increases were observed to go from 4 m^3/day to 12 m^3/day or so after 12 months of sand production from a heavy oil reservoir.

Interpreting foamy oil effects in terms of plastic radius propagation, Fig. 11 shows that there is little difference in the critical radius changes between foamy and non-foamy oil cases. This demonstrates that the mechanism is relatively independent of other rate enhancement mechanisms: foamy behavior lowers the pressure in the elastoplastic zone near the wellbore and creates more pressure drawdown farther out in the reservoir, even though the bottom-hole pressure near the wellbore changes little.

Model Simplifications and Limitations

In order to achieve semi-analytical solutions, some assumptions were made during model development, and these should be re-emphasized:

- All produced sand is assumed to come from the increase of critical radius and porosity in the elastoplastic zone;
- The deformation in the plastic zone is small so that compression effect can be neglected; and,
- Porosity and permeability in the elastoplastic zone are only functions of time;

Moreover, to investigate the variations of production rate, the bottom hole pressure is treated as a constant throughout the simulations, whereas in some previous work (e.g. Ref. 14), the well was subjected to a specific gradual drawdown strategy. A constant BHP may be viewed as a model limitation, but we believe that because the models are based on sound physics, adjustments and calibrations can be incorporated to give useful results in practice. Further developments in this analysis may also allow this to be treated semi-analytically. We note that in such a complex topic involving fluid and solid coupled behavior, an ability to quantitatively analyze heavy oil enhancement mechanisms during sand production involving a total of only 14 parameters (Table 2), all of which are usually available in the field, seems quite positive.

Conclusions

It is well recognized that oil enhancement from a CHOPS well is beyond the scope of conventional Darcy-based analysis of oil production. A set of models are developed, coupled, semi-analytically solved, and verified to quantify the contribution of each mechanism to oil enhancement in CHOPS. The mechanisms on which model development focused are porosity and permeability enhancement from sand extraction, outward propagation of the plastic zone radius, oil relative velocity increase from Darcy's law, and foamy oil behavior.

Preliminary calculations carried out with this model indicate several relationships.

- The improvement of formation transport properties such as porosity and permeability arising from sand removal plays a far more important role than the change of fluid relative velocity from Darcy's law in enhancing and sustaining long-term oil production.
- The propagation of the plastic zone, where low pressure and high permeability lead to a large-diameter wellbore effect, is identified as an important oil rate enhancement mechanism. It must be treated as at least as important as the increase of rock porosity and permeability in the rate enhancement observed in CHOPS.
- Foamy behavior, characterized as bubble growth, compressibility increase, and density reduction, make a significant difference in oil production rates. An enhancement factor of 3 is noted, compared to less than a doubling of oil rate without considering foamy oil effects. Furthermore, foamy behavior also lowers the pressure in the elastoplastic zone near the wellbore and creates more pressure drawdown in the reservoir.
- The calculations made reasonably match the production history as shown in Fig. 3, and this gives assurance that once the physical processes are correctly stipulated and captured in equations, predictions of rates involving CHOPS production can be developed.

These results facilitate the understanding of oil enhancement mechanisms during sand production. Because the model development was based on the physics of the processes, adjustments and calibrations can be easily incorporated to give useful predictive capabilities in practice. In a real field case, the early production history from a well can be used to predict future behavior, and the predicted production history from a field can be calculated on a similar basis.

Acknowledgement

This effort was supported in part by Terralog Technologies USA, Inc. and by the US Department of Energy, under contract DE-FG03-02ER83558.

NOMENCLATURE

B_f	=	fluid formation volume factor
c_f	=	fluid compressibility, 1/Pa
c_s	=	solid compressibility, 1/Pa
c_t	=	total compressibility, $\phi c_t = \phi c_f + (1-\phi)c_s$, 1/Pa
C_o	=	cohesive shear strength, Pa
CS_{ms}	=	accumulated sand mass, kg
CS	=	accumulated volume sand, m^3
E	=	Young's modulus, Pa
I_0	=	modified Bessel function of the first kind of the order zero
I_1	=	modified Bessel function of the first kind of the first order
k	=	permeability, Darcy
K_0	=	modified Bessel function of the second kind of the order zero

K_1	=	modified Bessel function of the second kind of the first order
m_f	=	fluid mass velocity, kg/s
P_{fsat}	=	fluid saturation pressure, Pa
P_p	=	pressures in plastic zone, Pa
P_e	=	pressures in elastic zone, Pa
P_c	=	pressure at the critical radius, Pa
$\overline{P_p}$	=	Laplace transform of P_p, dimensionless
$\overline{P_e}$	=	Laplace transform of P_e, dimensionless
q_s	=	volumetric solid rate per unit thickness of reservoir, m^2/s
q	=	volumetric oil rate per unit thickness of reservoir, m^2/s
q_o	=	initial oil production rate before sanding occurs, m^2/s
q_{sc}	=	volumetric production rate at surface condition, m^2/s
Q_s	=	sanding volume rate, m^3/s
Q	=	oil volume rate, m^3/s
Q_{ms}	=	sanding mass rate, kg/s
Q_{mso}	=	initial sanding mass rate, kg/s
r	=	radius from wellbore, m
R_1	=	wellbore radius, m
R_2	=	outer radius, m
R_c	=	critical radius, m
s	=	Laplace parameter
t	=	time since sanding starts, s
v_f	=	fluid velocity, m/s
v_s	=	solid velocity, m/s
β	=	failure angle, radius
ϕ	=	rock porosity in the plastic zone
ϕ_i	=	rock porosity in the plastic zone
φ	=	friction angle, radian
σ'_r	=	effective radial stress, Pa
σ'_θ	=	effective tangential stress, Pa
μ	=	oil viscosity, Pa·s
ν	=	Poisson's ratio

REFERENCES

1. Smalley, C., Heavy oil and viscous oil, *Modern Petroleum Technology, John Wiley & Sons Ltd., 2000.*
2. World Energy Council: Survey of Energy Resources. London, UK, 1998.
3. Kobbe, W., AIME New York Meeting, *Trans. AIME, Vol. LVI, 814, Feb. 1917.*
4. Smith, G.E., Fluid flow and sand production in heavy oil reservoirs under solution gas drive; *paper SPE 15094, the 56th SPE California Regional Meeting*, *Oakland, CA, 2-4 Apr. 1986.*
5. Dusseault, M.B., and El-Sayed, S., CHOP – Cold Heavy Oil Production; *Proc. 10th European Improved Oil Recovery Symp. EAGE, Brighton, Aug. 1999.*
6. Vaziri, H.H., Lemoine, E., Palmer, I.D., and McLennan, J. et al., How can sand production yield a several-fold increase in productivity: experimental and field data; *paper SPE 63235, the 2000 SPE Annual Technical Conference and Exhibition, Dallas, TX, 1-4 Oct. 2000.*
7. Palmer, I., McLennan, J., and Vaziri, H., Cavity-like completions in weak sands*; paper SPE 58719, SPE International Symposium on Formation Damage Control, Lafayette, LA, 23-24 Feb. 2000.*
8. Geilikman, M.B., and Dusseault, M.B., Sand production caused by foamy oil flow; *Transport in Porous Media, Vol. 35, pp. 259-272.*
9. Dusseault, M.B., New Oil Production Technologies; *the SPE Distinguished Lecture Series, Calgary, AB, Canada, 2003.*
10. Bora, R., Maini, B.B., and Chakma, A., Rheology of foamy oil in porous media; *the 7th Saskatchewan Petroleum Conference, Regina, SK, Canada, 20-22 Oct. 1997.*
11. Huerta, M., Otero, C., Rico, A., and Jiménez, I. et al., Understanding foamy oil mechanisms for heavy oil reservoirs during primary production; *paper SPE 36749, SPE Annual Technical Conference and Exhibition, Denver, CO, 6-9 Oct. 1996.*
12. Sarma, H.K., and Maini, B.B., Role of solution gas in primary production of heavy oils; *Paper SPE 23631, SPE Latin Conference, Caracas, Venezuela, 6-11 Mar. 1992.*
13. Ehlig-Economides, C.A., Fernandez, B.G., and Gongora, C.A., Global experiences and practice for cold production of moderate and heavy oil; *paper SPE 58773, SPE International Symposium on Formation Damage Control, Lafayette, LA, 23-24 Feb. 2000.*
14. Geilikman, M.B., and Dusseault, M.B., Fluid rate enhancement from massive sand production in heavy-oil reservoirs; *J. Pet. Sci & Eng., Vol. 17, pp5-18, 1997.*
15. Wang, Y., Chen, C., and Dusseault, M.B., An integrated reservoir model for sand production and foamy oil flow during cold heavy oil production, *paper SPE 69714, SPE Intl. Thermal Operations and Heavy Oil Symp., Margarita, Venezuela, 12-14 March, 2001.*
16. Dusseault, M.B., and Santarelli, F. J., A conceptual model for massive solids production in poorly consolidated sandstone; *Proc. the Intl. Symp. on Rock at Great Depth, A.A.Balkema, Rotterdam, 789-797, 1989.*
17. Vaziri, H.H, Phillips, R., and Hurley, S., Physical modeling of sand production; *Intl. J. Rock Mech. & Min Sci. Vol. 34, No.3-4, p323, 1999.*
18. Tremblay, B., Sedgwick, G., and Vu, D., A review of cold production in heavy oil production; *the EAGE-10th European Symp. on Improved Oil Recovery, Brighton, UK, Aug. 1999.*
19. Bruno, M.S., Bovberg, C.A., and Meyer, R.F., Some influences of saturation and fluid flow on sand production: laboratory and discrete element model investigations; *paper SPE 36534, SPE Annual Technical Conference and Exhibition, Denver, CO, 6-9 October, 1996.*
20. Papamichos, E., and Malmanger, E.M., A sand erosion model for volumetric sand predictions in a North Sea reservoir; *paper SPE 54007, the SPE Latin American and Caribbean Petroleum Engineering Conference, Caracas, Venezuela, 21-23 Apr. 1999.*
21. Dullien, F.A.L., Porous Media: Fluid Transport and Pore Structure; *Academic Press, New York, 1979*.
22. Dusseault, M.B., and El-Sayed, S., Heavy oil well production enhancement by encouraging sand influx; *paper SPE 59276, the SPE/DOE Improved Oil Recovery Symposium, Tulsa, OK, 3-5 April, 2000.*
23. Han, G., and Dusseault, M.B., Description of fluid flow around a wellbore with stress-dependent porosity and permeability; *J. Pet. Sci & Eng. Vol. 40, No.1-2, pp.1-16, 2003.*

24. Carslaw, H.S., and Jaeger, J.C., Conduction of Heat in Solids; *2nd edition, Oxford University Press, Oxford, UK, 1959.*

25. Stehfest, H., Numerical inversion of Laplace transforms; *Communications of the ACM, Vol. 13, No.1, pp.47-49, 1970.*

26. Wong, F.Y., and Ogrodnick, W.P., Redevelopment of heavy oil assets through technology advances; *Proc. the 7th UNITAR Conf on Heavy Oil and Tar Sands, Beijing, P. R. China, Manuscript No.211, 1953-1966, 1998.*

Appendix A: Elastic Stresses and R_c

For steady-state fluid flow, the elastic stresses can be expressed as [23]:

$$\sigma_r^{'} = -\frac{0.5}{1-\nu}P + \frac{Ec_1}{(1+\nu)(1-2\nu)} - \frac{Ec_2}{(1+\nu)}\frac{1}{R_c^{\,2}} - \frac{0.5-\nu}{1-\nu}\frac{\overline{q}}{2} \quad ...(A\text{-}1)$$

$$\sigma_\theta' = -\frac{0.5}{1-\nu}P + \frac{Ec_1}{(1+\nu)(1-2\nu)} + \frac{Ec_2}{(1+\nu)}\frac{1}{r^2} + \frac{0.5-\nu}{1-\nu}\cdot\frac{\overline{q}}{2} \quad ...(A\text{-}2)$$

where $\overline{q} = \dfrac{q\mu}{2\pi k_i}$.

Assuming radial stresses are continuous across the interface between the elastic and plastic zones:

$$\frac{c_3}{\omega}R_c^{\,-\omega} + \frac{2C_o\tan\beta + \Gamma(t)}{\omega} = -\frac{0.5}{1-\nu}P_c + \frac{Ec_1}{(1+\nu)(1-2\nu)} - \frac{Ec_2}{(1+\nu)}\frac{1}{R_c^{\,2}} - \frac{0.5-\nu}{1-\nu}\frac{\overline{q}}{2} \quad .....(A\text{-}3)$$

$$\frac{c_3(1-\omega)}{\omega}R_c^{\,-\omega} + \frac{2C_o\tan\beta + (1-\omega)\Gamma(t)}{\omega} = -\frac{0.5}{1-\nu}P_c + \frac{Ec_1}{(1+\nu)(1-2\nu)} + \frac{Ec_2}{(1+\nu)}\frac{1}{R_c^{\,2}} + \frac{0.5-\nu}{1-\nu}\frac{\overline{q}}{2} \quad .....(A\text{-}4)$$

where P_c is pore pressure at R_c and can be expressed as

$$P_c = P_2 - \overline{q}\ln\left(\frac{R_2}{R_c}\right)$$

Another boundary condition used is the assumption that in the far field the effective radial stress is equal to the horizontal effective stress (i.e. $\sigma'_r(R_2) = \sigma'_h$):

$$\frac{Ec_1}{(1+\nu)(1-2\nu)} - \frac{0.5}{1-\nu}P_2 - \frac{Ec_2}{(1+\nu)}\frac{1}{R_2^{\,2}} - \frac{0.5-\nu}{1-\nu}\frac{\overline{q}}{2} = \sigma'_h \quad ....(A\text{-}5)$$

Finally, the three unknown constants R_c, c_1, c_2, in the above three equations can be solved:

$$c_1 = \frac{(1+\nu)(1-2\nu)}{E}(\sigma'_h + \frac{0.5}{1-\nu}P_2 + \frac{Ec_2}{(1+\nu)}\frac{1}{R_2^{\,2}} + \frac{0.5-\nu}{1-\nu} \quad ..(A\text{-}6)$$

$$c_2 = -\frac{1+\nu}{2E}(\frac{0.5-\nu}{1-\nu}\overline{q} + \Gamma(t) + c_3R_c^{\,-\omega})\cdot R_c^2 \quad .....(A\text{-}7)$$

$$2\sigma'_h - \frac{4C_o\tan\beta + (2-\omega)\Gamma(t)}{\omega} + \frac{0.5-\nu}{1-\nu}\overline{q} = \frac{c_3(2-\omega)}{\omega}R_c^{\,-\omega} + \frac{\overline{q}}{1-\nu}\ln\left(\frac{R_c}{R_2}\right) + \left(\frac{0.5-\nu}{1-\nu}\overline{q} + \Gamma(t) + c_3R_c^{\,-\omega}\right)\frac{R_c^{\,2}}{R_2^{\,2}} \quad .....(A\text{-}8)$$

Eq. (A-8) is a nonlinear equation of R_c, in the form of $f(R_c^{-\omega}, R_c^2, \ln(R_c)) = 0$, which can be easily solved with the aid of mathematical software (e.g. Matlab).

Appendix B: Solution for Foamy Oil Pressure

Applying Laplace transformation to Eqs. (20) and (21) in cylindrical coordinates:

$$\frac{d^2\overline{P}_p^{\,(1+B_f)}}{dr^2} + \frac{1}{r}\frac{d\overline{P}_p^{\,(1+B_f)}}{dr} - \chi^2\overline{P}_p^{\,(1+B_f)} = 0 \quad .....(B\text{-}1)$$

$$\frac{d^2\overline{P}_e^{\,(1+B_f)}}{dr^2} + \frac{1}{r}\frac{d\overline{P}_e^{\,(1+B_f)}}{dr} - \chi_i^{\,2}\overline{P}_e^{\,(1+B_f)} = 0 \quad .....(B\text{-}2)$$

where $\chi = \sqrt{s/M}$, $\chi_i = \sqrt{s/M_i}$, and s is the Laplace parameter. If the outer boundary R_2 is treated as infinity, the solutions of above equations can be found in forms of [24]

$$\overline{P}_p^{\,(1+B_f)} = AI_0(\chi r) + BK_0(\chi r) \quad .....(B\text{-}3)$$

$$\overline{P}_e^{\,(1+B_f)} = CK_0(\chi_i r) \quad .....(B\text{-}4)$$

where I_0, K_0 are the modified Bessel function of the first kind and the second kind, respectively, of order zero. A, B, C are functions of the Laplace operator s, and they are chosen so that $\overline{P}_p$ and $\overline{P}_e$ satisfy the transforms of the boundary conditions

$$\overline{P}_p\big|_{r=R_1} = \frac{P_1}{s} \quad .....(B\text{-}5)$$

$$\overline{P}_p\big|_{r=R_c} = \overline{P}_e\big|_{r=R_c} \quad .....(B\text{-}6)$$

$$k\frac{\partial\overline{P}_p^{\,1+B_f}}{\partial r}\bigg|_{r=R_c} = k_i\frac{\partial\overline{P}_e^{\,1+B_f}}{\partial r}\bigg|_{r=R_c} \quad .....(B\text{-}7)$$

Substituting Eqs. B-3 and B-4 into the above conditions, A, B, C can be solved as

$$B = \frac{\left[\Pi_{10} + \overline{\mathrm{K}}\Pi_{00}\right]\frac{P_1^{(1+B_f)}}{s}}{K_1(\chi R_c) + \Pi_{10}K_0(\chi R_1) - \overline{\mathrm{K}}\left[K_0(\chi R_c) - K_0(\chi R_1)\right]}$$

$$A = \frac{1}{I_0(\chi R_1)}\left[\frac{P_1^{(1+B_f)}}{s} - BK_0(\chi R_1)\right]$$

$$C = \frac{1}{K_0(\chi_i R_c)}\left\{\left[K_0(\chi R_c) - \Pi_{00}K_0(\chi R_1)\right]B + \Pi_{00}\frac{P_1^{(1+B_f)}}{s}\right\} \quad .....(B\text{-}8)$$

where $\overline{\mathrm{K}} = \dfrac{k_i\chi_i}{k\chi}\dfrac{K_1(\chi_i R_c)}{K_0(\chi_i R_c)}$, $\Pi_{10} = \dfrac{I_1(\chi R_c)}{I_0(\chi R_1)}$, $\Pi_{00} = \dfrac{I_0(\chi R_c)}{I_0(\chi R_1)}$.

It would involve prohibitive mathematical efforts to analytically invert the above Laplace transforms. Numerically,

the Stehfest method is widely applied because of its simplicity [25]. If $\overline{P}(r,s)$ is the Laplacian, then the inverse (i.e. the original function) $P(r,t)$ can be approximately calculated by

$$P(r,t) = \frac{\ln 2}{t}\sum_{i=1}^{N} V_i \overline{P}(r, \frac{i \ln 2}{t}) \quad \text{(B-9)}$$

where $\ln 2/t$ substitutes for the Laplace parameter s, and the coefficients V_i are

$$V_i = (-1)^{N/2+i} \sum_{k=(i+1)/2}^{\min(i,N/2)} \frac{k^{N/2}(2k)!}{(N/2-k)!k!(k-1)!(i-k)!(2k-i)!} \quad \text{(B-10)}$$

where N is an even number. The magnitude of the error is of order $((N/2)!)^{-1}$.

Tables

Table 1. Sand production history

Sanding Time (month)	Density of sands (kg/m^3)	Initial sanding rate (m^3/day)	Final sanding rate (m^3/day)	Sanding rate at 6th month (m^3/day)
12	2.65	0.6	0.12	0.20

TABLE 2. Parameters used in models

ϕ_i	k_i (Darcy)	Q (m^3/day)	μ (Pa.s)	R_1 (m)	R_2 (m)	h (m)	P_2 (MPa)	P_{sat} (MPa)	E (GPa)	ν	σ_h (MPa)	C_o (MPa)	φ
0.32	3	3.98	1	0.1	100	10	10	3.4	3	0.3	28	0.5	30^o

Figures

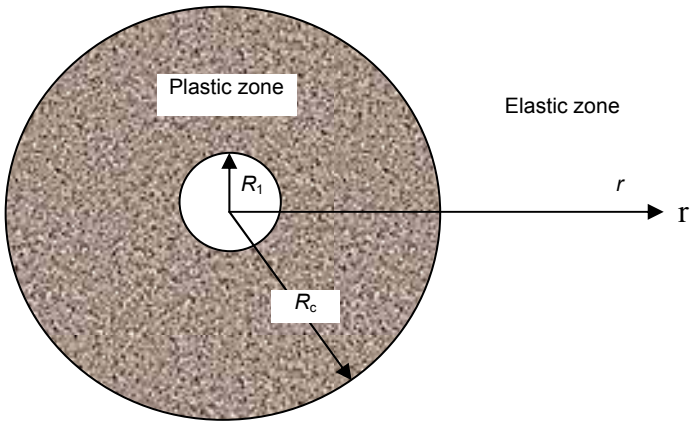

Fig. 1: Conceptual model for theoretical development

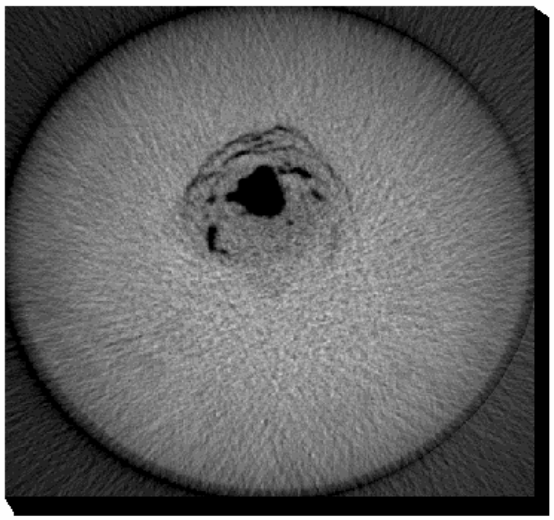

Fig. 2: Experimental observation of a rock sample after sanding (after Bruno *et al.*[19])

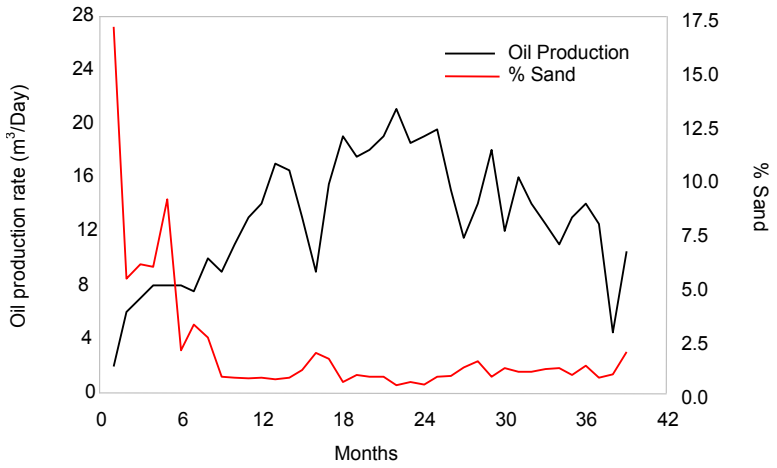

Fig. 3: Field data of CHOPS (after Wong and Ogrodnick [26])

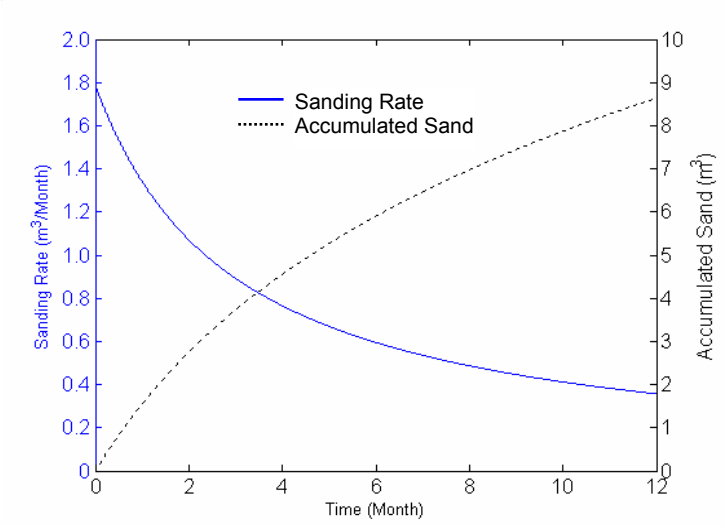

Fig. 4: Sand production history

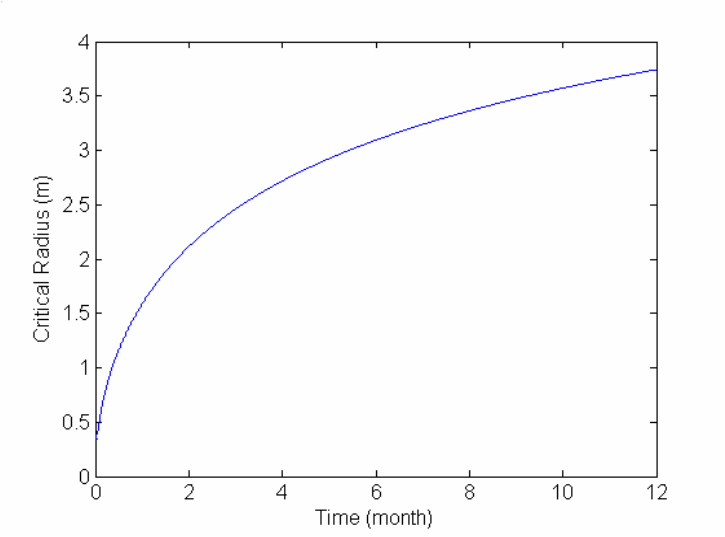

Fig. 5: Evolution of critical radius during CHOPS

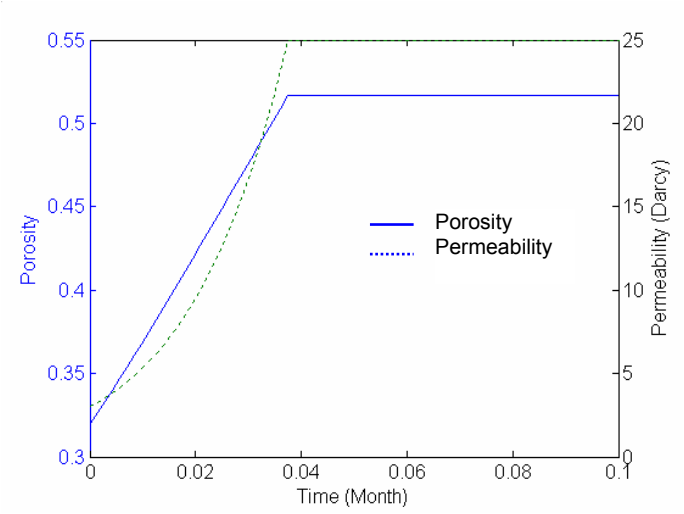

Fig. 6: Evolution of porosity and permeability during CHOPS

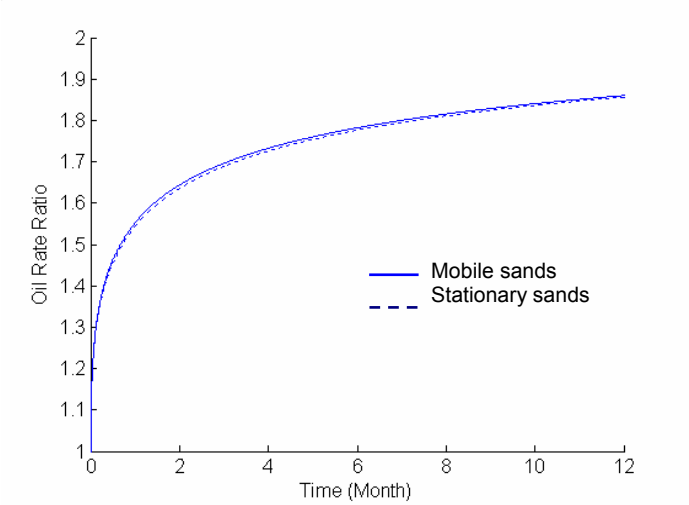

Fig. 7: Effect of sand movement on oil production

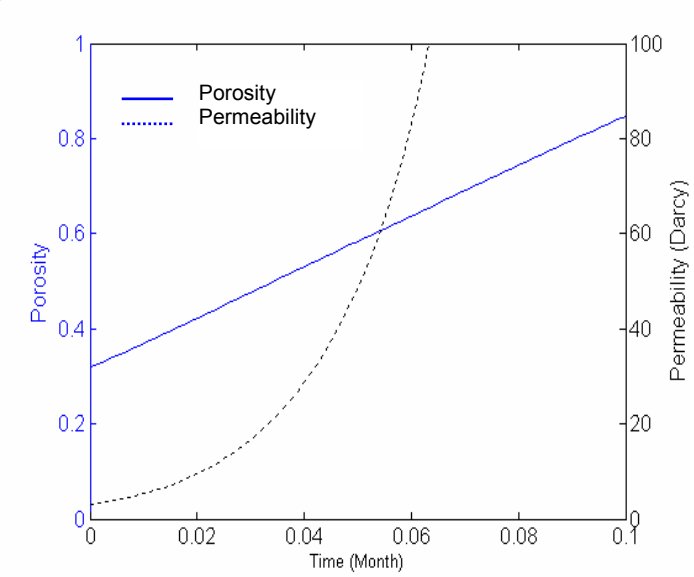

Fig. 8: Evolution of porosity and permeability (without porosity cap)

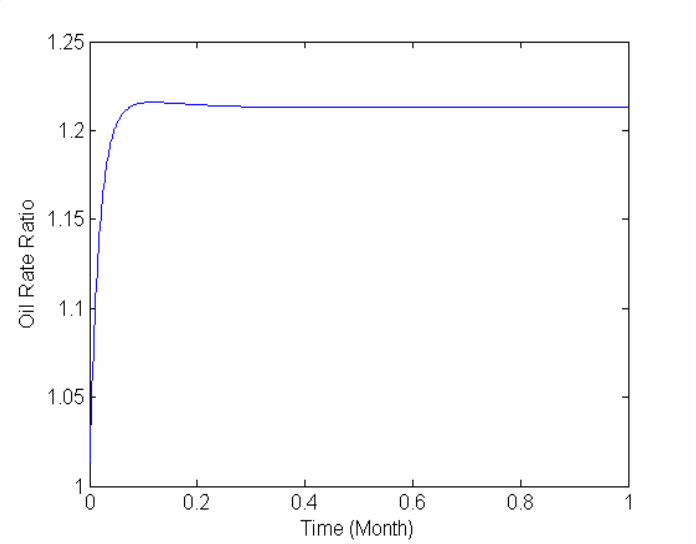

Fig. 9: Enhanced oil rate by sand movement (without porosity cap)

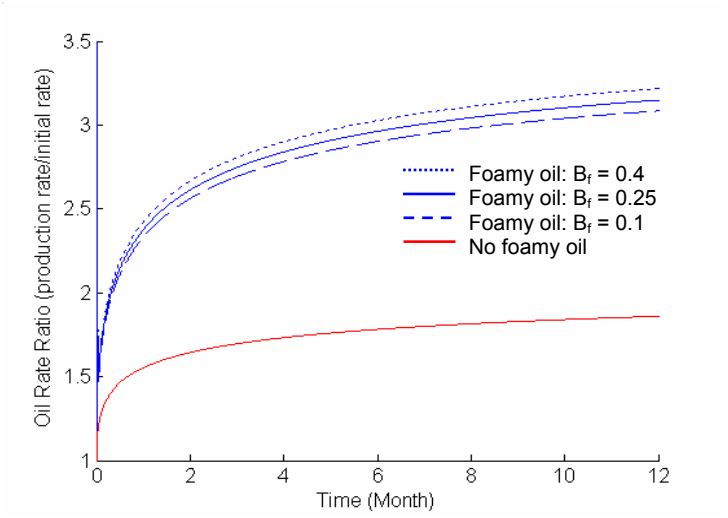

Fig. 10: Effect of sand production and foamy oil behavior on oil production

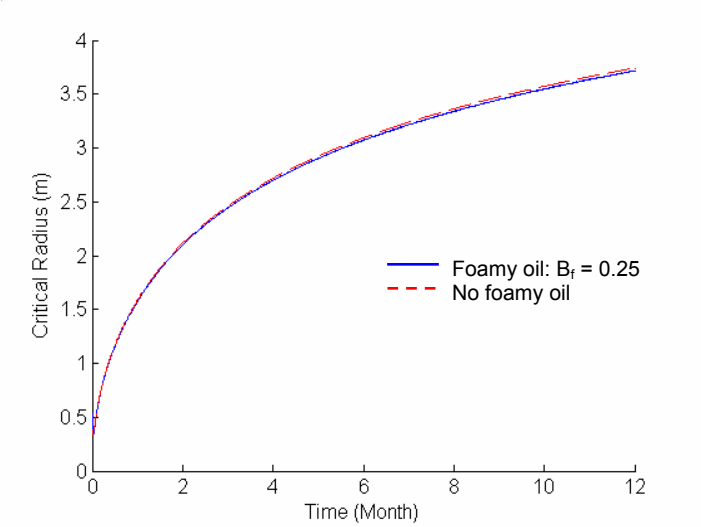

Fig. 11: Effect of sand production and foamy oil behavior on plastic zone